

Evolution of the Ceramic Structure during Thermal Degradation of a Si–Al–C–O Precursor

Xudong Li and Mohan J. Edirisinghe*

Department of Materials, Queen Mary, University of London, Mile End Road,
London E1 4NS, UK

Received August 1, 2003. Revised Manuscript Received December 4, 2003

Solid-state magic angle spinning nuclear magnetic resonance (MAS NMR), X-ray diffraction (XRD), and scanning electron and transmission electron microscopy (SEM and TEM) are used to study thermal degradation of a Si–Al–C–O ceramic precursor in nitrogen. A polysilane (PS) and aluminum acetylacetonate (AlAce) in the weight ratio AlAce/PS = 2 were reacted to synthesize the precursor. Solid state ^{29}Si and ^{27}Al MAS NMR spectra of the precursor confirm the occurrence of chemical reactions between PS and AlAce during synthesis. A complete three-dimensional Si–O–Al network forms at 900 °C. Crystalline phases appear at 1300 °C, and the pyrolyzed product at 1700 °C is a solid solution of 2H–SiC and AlN. Solid state ^{29}Si and ^{27}Al MAS NMR and XRD provide detailed information about the phase formation and transformation. The morphological development and microstructure evolution are further characterized by SEM and TEM.

Introduction

The development of innovative chemical routes for the preparation of advanced ceramics is a current key research topic. In contrast to the mechanical mixing and grinding of powdered solids used in conventional ceramic processing methods, chemical synthesis is capable of achieving molecular level homogeneity of the starting materials. Therefore, chemical processing routes have significant advantages, for example, the easy composition control, feasible preparation of materials of metastable phases or with narrow sintering temperature (hard to achieve using powdered solid-state reactions), the reduction of sintering temperature, and an improved consistency of the final products.^{1–6} These are very attractive for fabrication of multicomponent nanocomposite covalent ceramics, which are hard to fabricate because of their low solid-state interdiffusivities.

Since the pioneering work of Yajima in 1975, which led to the first commercial ceramic fibers from polysilane,⁷ the polymeric precursor route for the synthesis of covalently bonded ceramics such as Si_3N_4 , AlN, and BN has been researched extensively. The preparation of composite ceramics, using single source precursors or simply by mixing different precursors of component

materials, has also gained increasing interest.^{1–4,8–10} For example, SiC–AlN ceramics, which form extensive solid solutions¹¹ and have promising applications as high-temperature structural ceramic materials and electronic materials, have continuously received a great deal of attention. Interrante and co-workers^{2–4} prepared SiC–AlN ceramics by pyrolysis of mixtures of several organosilicon and organoaluminum compounds. Their work confirmed that the molecular level homogeneity attained in the initial precursor mixtures was maintained in the pyrolyzed ceramic products. More recently, Boury and Seyferth⁹ obtained SiC–AlN ceramics by pyrolysis of polyaluminasilazane, and Nakashima et al.¹⁰ studied the conversion of the precursor derived from cage-type and cyclic molecular building blocks into Al–Si–N–C ceramic composites.

The present authors¹² recently reported the controlled formation of SiC–AlN ceramics by pyrolysis of chemically modified polysilane with aluminum acetylacetonate (AlAce). The reaction of polycarbosilane with metallic alkoxide compounds is believed to be an efficient route to introduce heteroatoms. The Si–Ti–C–O, Si–Zr–C–O, and Si–Al–C–O fibers prepared in this way have shown improved heat-resistance.^{13–15} Advanced ceramics such as SiC/ZrC, SiC/TiC, SiC/Al₂O₃, and β' -sialon have also been prepared.^{15–18}

* To whom correspondence should be addressed. Phone: +44 (0)20 7882 7767. Fax: +44 (0)20 8981 9804. E-mail: m.j.edirisinghe@qmul.ac.uk.

(1) Seyferth, D.; Wiseman, G. H. *J. Am. Ceram. Soc.* **1984**, *67*, C132.
(2) Interrante, L. V.; Czekaj, C. L.; Hackney, M. L. J.; Sigel, G. A.; Shields, P. J.; Slack, G. A. *Mater. Res. Soc. Symp. Proc.* **1988**, *121*, 465.
(3) Czekaj, C. L.; Hackney, M. L. J.; Hurley, W. J., Jr.; Interrante, L. V.; Sigel, G. A.; Shields, P. J.; Slack, G. A. *J. Am. Ceram. Soc.* **1990**, *73*, 352.
(4) Interrante, L. V.; Schmidt, W. R.; Marchetti, P. S.; Maciel, G. E. *Mater. Res. Soc. Symp. Proc.* **1992**, *271*, 739.
(5) BonhommeCoury, L.; Babonneau, F.; Livage, J. *Chem. Mater.* **1993**, *5*, 323.
(6) Gerardin, C.; Sundaresan, S.; Benziger, J.; Navrotsky, A. *Chem. Mater.* **1994**, *6*, 160.
(7) Yajima, S.; Hayashi, J.; Omori, M. *Chem. Lett.* **1975**, 931.

(8) Löffelholz, J.; Jansen, M. *Adv. Mater.* **1995**, *7*, 289, 292.
(9) Boury, B.; Seyferth, D. *Appl. Organomet. Chem.* **1999**, *13*, 431.
(10) Nakashima, H.; Koyama, S.; Kuroda, K.; Sugahara, Y. *J. Am. Ceram. Soc.* **2002**, *85*, 59.
(11) Zangvil, A.; Ruh, R. *J. Am. Ceram. Soc.* **1988**, *71*, 884.
(12) Li, X. D.; Edirisinghe, M. J. *Proc. R. Soc. London A* **2003**, *459*, 2731.
(13) Yajima, S.; Iwai, T.; Yamamura, T.; Okamura, K.; Hasegawa, Y. *J. Mater. Sci.* **1981**, *16*, 1349.
(14) Ishikawa, T.; Kohtoku, Y.; Kumagawa, K.; Yamamura, T.; Nagasawa, T. *Nature* **1998**, *391*, 773.
(15) Yamaoka, H.; Ishikawa, T.; Kumagawa, K. *J. Mater. Sci.* **1999**, *34*, 1333.
(16) Babonneau, F.; Sorarù, G. D.; Mackenzie, J. D. *J. Mater. Sci.* **1990**, *25*, 3664.

Polysilane (PS) used in this study is an organosilicon polymer for SiC with the Si–Si backbone structure. An enhanced oxycarbide formation was reported to be achieved due to the reactivity of Si–Si bonds.¹⁹ PS chemically reacts with AlAce to form a family of Si–Al–C–O precursors and this leads to an improved pyrolysis yield.¹² Compared with the general metal–nonmetal bonds of organometallic compounds, the simultaneous existence of heterometallic M–O–M' bonds also occurs in Si–Al–C–O precursors via addition of AlAce, and their relative content would vary according to the initial AlAce/PS ratio. Therefore, the thermal degradation of Si–Al–C–O precursors is expected to proceed via crystallization of SiC from SiC₄ moieties, derived from PS, and/or carbothermal reduction and simultaneous nitridation when a higher amount of AlAce is added to polysilane.

In the present study, the Si–Al–C–O precursor with AlAce/PS = 2.00 was thermally degraded in nitrogen to ceramics in stages in order to investigate the changes in the local coordination environments of both Si and Al atoms, phase formation and transformation, and microstructural evolution.

Experimental Procedure

Preparation of Si–Al–C–O Precursor. The PS used was synthesized using Wurtz alkali metal condensation of a chlorinated silane combination (dichloromethylphenylsilane/dichloromethylvinylsilane/trichlorophenylsilane molar ratio 0.6:0.2:0.2).²⁰ PS and AlAce were dissolved, AlAce/PS = 2.00 (by weight), in toluene by mixing to form a homogeneous solution. After reflux reaction for 2 h in a flowing nitrogen protective atmosphere, the solution was heated to 250 °C to distill off the solvent. The residue was then concentrated at ~320 °C for 3 h to give a solid, which is the Si–Al–C–O precursor (real Al/Si molar ratio of ca. 0.48). The precursor was powdered and used in pyrolysis experiments.

Pyrolysis. Pyrolysis was carried out in a tube furnace in flowing nitrogen gas. The samples were placed in alumina crucibles and heated at 5 °C min⁻¹ to the designated temperature and soaked as stated below, followed by furnace cooling to the ambient temperature. For structural evaluation at ≤900 °C, the precursor was soaked at 500, 700, and 900 °C, respectively, for 2 h. The precursor pyrolyzed at 900 °C was used further as *source powder*, which was heated to 1100, 1300, 1500, and 1700 °C and soaked at each final temperature for 40 min.

The crucibles loaded with samples were weighed before and after pyrolysis so that sample weight changes were recorded. An empty crucible was weighed and used as a control for calibration of pyrolysis at each designated temperature.

Measurements. Solid-state nuclear magnetic resonance (NMR) spectra of the pyrolyzed products were obtained on a Bruker MSL300 spectrometer (7.05 T) at 59.6 MHz (²⁹Si) and 78.2 MHz (²⁷Al) using standard Bruker double-resonance magic-angle sample spinning (MAS) probes. ²⁹Si spectra were recorded by spinning powdered samples at a MAS frequency of 5.5 kHz, using both cross-polarization (CP) and single-pulse (SP) experiments. Typical operating conditions for ²⁹Si CP/MAS were ¹H 90° pulse duration = 5.5 μs, contact time = 2 ms, and recycle delay = 1 s. Conditions for ²⁹Si SP/MAS experiments were ²⁹Si 30° pulse duration = 1.7 μs and recycle

delay = 60 s. ²⁹Si NMR spectra were processed using 1024 data points zero filling to 8192, with 50 Hz line broadening, whereas 100 Hz line broadening was applied for the pyrolysis ≥900 °C. In ²⁷Al MAS NMR measurements, the spinning rate was 12.0 kHz. High-resolution ²⁷Al spectra were recorded using a pulse duration of 0.7 μs with a recycle delay of 1.0 s. Typical spectra consisting of 9500 scans, acquired at a spectral width of 125 kHz, were processed using 2048 data points zero filling to 8192. No line-broadening was applied prior to Fourier transformation. High-power ¹H decoupling is always applied during acquisition. The ²⁹Si and ²⁷Al chemical shifts are referenced to tetramethylsilane and 1 M aqueous Al(NO₃)₃, which are assigned to 0 ppm. The Dmfit program was used for ²⁹Si spectral deconvolutions.²¹

The X-ray powder diffraction (XRD) patterns of the pyrolyzed products were recorded using an automated Philips PW 1050/30 X-ray diffractometer with Cu Kα radiation and a Ni filter. Working conditions were 40 kV and 30 mA. Data were collected in the range of 2θ = 10–90° with 0.05-s step width, 2-s scan time, and 1-s delay time.

The microstructures of the pyrolyzed products were examined using a scanning electron microscope (JEOL 6300, accelerating voltage 15 kV) and a transmission electron microscope (JEOL 2010, accelerating voltage 200 kV). Composition microanalysis was performed using an Oxford Incan energy-dispersive X-ray (EDX) system attached to the electron microscopes and thereby the actual Al/Si ratios of the samples were estimated. In the case of SEM, a thin layer of gold was coated on samples, and for TEM investigations the samples were dispersed in pure alcohol and then collected using lacey microscope grids coated with carbon film.

Results

Pyrolysis ≤ 900 °C. ²⁹Si MAS NMR. Both CP/MAS and SP/MAS experiments were used for evaluation of the Si local coordination environments of the precursor and those pyrolyzed at temperatures ≤900 °C. Figure 1 includes ²⁹Si spectra of the precursor and the samples pyrolyzed at 500 and 700 °C, recorded using CP/MAS sequence, while the spectra of the samples pyrolyzed at 700 and 900 °C collected using SP/MAS sequence are also shown.

The CP/MAS spectrum of the precursor (Figure 1a) gives three separate resonance signals, characteristic of SiC₀ species.^{22–24} The strongest peak with the maximum at –65.6 ppm is assigned to tetrahedral Si sites with three oxygen neighbors (SiC₀–T type, 40.2%). The peak at –19.7 ppm is attributable to Si sites with two oxygen neighbors (SiC₂O₂–D type, 22.0%). The two identified components in its downfield direction, at 10.3 ppm and at –2.9 ppm, are assigned to Si sites with one oxygen neighbor (SiC₃O–M type, 13.0%) and SiC₄ (14.2%) sites, respectively. The resonance signal centered at –104.0 ppm is ascribed to the Si sites with four oxygen neighbors (SiO₄–Q type, 10.6%). At 500 °C, the resonances for types M and D sites and the SiC₄ sites decrease significantly. Instead, Q type sites grow significantly and shift to –93.1 ppm. At 700 °C, signals from types M and D sites and SiC₄ sites were not

(21) Massiot, D.; Fayon, F.; Capron, M.; King, I.; Le Calvé, S.; Alonso, B.; Durand, J.-O.; Bujoli, B.; Gan, Z.; Hoatson, G. *Magn. Reson. Chem.* **2002**, *40*, 70.

(22) Marsmann, H. In *NMR Basic Principles and Progress*; Diehl, P., Fluck, E., Kosfeld, R., Eds.; Springer-Verlag: Berlin, 1981; Vol. 17, pp 65–235.

(23) Burns, G. T.; Taylor, R. B.; Xu, Y.; Zangvil, A.; Zank, G. A. *Chem. Mater.* **1992**, *4*, 1313.

(24) Babonneau, F.; Thorne, K.; Mackenzie, J. D. *Chem. Mater.* **1989**, *1*, 554.

(17) Babonneau, F.; Sorarù, G. D.; Thorne, K. J.; Mackenzie, J. D. *J. Am. Ceram. Soc.* **1991**, *74*, 1725.

(18) Sorarù, G. D.; Mercadini, M.; Maschio, R. D.; Taulelle, F.; Babonneau, F. *J. Am. Ceram. Soc.* **1993**, *76*, 2595.

(19) Belot, V.; Corriu, R. J. P.; Leclercq, D.; Mutin, P. H.; Vioux, A. *J. Non-Cryst. Solids* **1992**, *144*, 287.

(20) Bao, X.; Edirisinghe, M. J.; Fernando, G. F.; Folkes, M. J. *J. Eur. Ceram. Soc.* **1998**, *18*, 915.

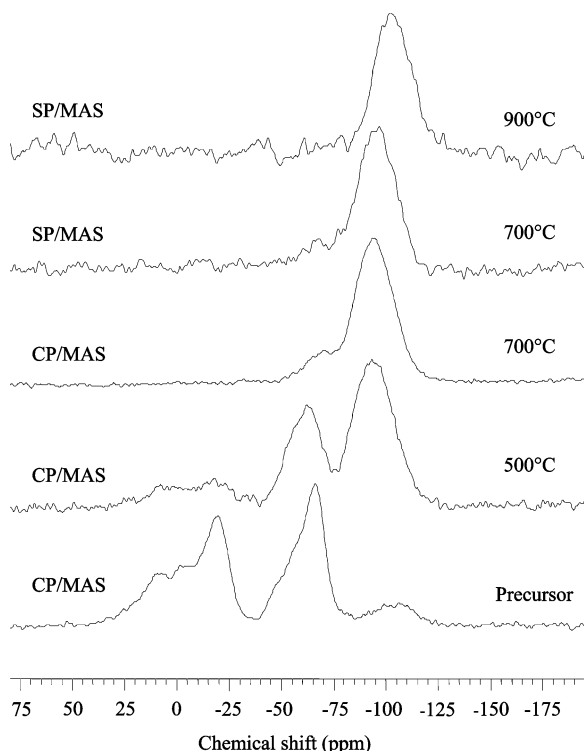


Figure 1. Solid-state ^{29}Si CP/MAS and SP/MAS NMR spectra of the precursor and samples pyrolyzed at 500, 700, and 900 °C.

recorded. The Q type sites at -93.9 ppm are a predominate resonance. The weak shoulder at -67.8 ppm is assigned to T type sites, which are located at -61.6 ppm at 500 °C.

The SP/MAS sequence recorded a spectrum similar to that of the CP/MAS experiment at 700 °C, confirming the existence of protons distributed homogeneously around the Si sites. The Q type sites in the SP/MAS spectrum are centered at -95.8 ppm. The upfield shift (ca. ~ 2 ppm) compared with the CP/MAS spectrum is presumably due to the deprotonation reaction. A strong peak centered at -101.0 ppm is the only resonance signal recorded at 900 °C, indicating the upfield shifting of Q type sites and the complete disappearance of other Si sites.

^{27}Al MAS NMR. In AlAce, Al is coordinated rather symmetrically by six oxygens from three acetylacetonate ligands. Its NMR gives a sharp single resonance near the origin.²⁵ Three peaks are observed in the precursor (Figure 2), located at -3.8 , 27.6 , and 53.0 ppm, and assigned to AlO_6 , AlO_5 , and AlO_4 sites, respectively.^{26–29} The pyrolysis of the precursors leads to a relative increase in the peak intensities of AlO_4 and AlO_5 species.

AlO_6 sites are the most intensive in the precursor. The shifting of Al atoms to AlO_4 and AlO_5 sites occurs when the temperature is elevated. AlO_5 sites significantly gain

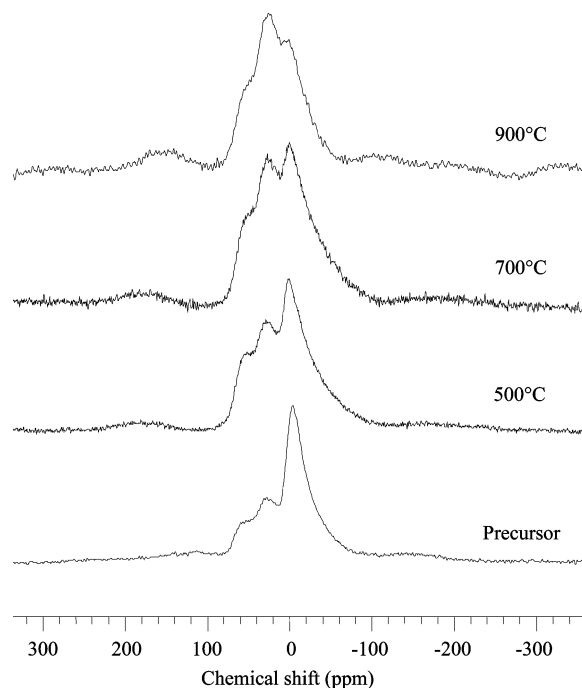


Figure 2. Solid-state ^{27}Al MAS NMR spectra of the precursor and samples pyrolyzed at 500, 700, and 900 °C.

in intensity relative to AlO_4 at 700 °C and even become the most intensive at 900 °C. The pentacoordinated AlO_5 sites as intermediate environments are extensively associated with aluminosilicates and other Al-based precursors prepared using chemical routes.^{6,26–29} Corriu et al.²⁷ concluded that the presence of AlO_5 coordinations indicated the high homogeneity of aluminosilicate networks prepared by the non-hydrolytic process. Furthermore, AlO_5 sites are believed to be critical to the low-temperature direct mullitization of amorphous mullite-type materials.⁶ In addition, the presence of AlO_5 environments was also reported to aid the incorporation of nitrogen during heat treatment in NH_3 .²⁹

Pyrolysis up to 1700 °C. XRD. XRD patterns of the source powder and those pyrolyzed at different temperatures are given in Figure 3. The source powder and that pyrolyzed at 1100 °C give a broad diffuse hump at around $2\theta = 22.5^\circ$, confirming an amorphous structure. The onset of crystallization appears at 1300 °C but the exact crystalline phase cannot be deduced by XRD patterns alone due to the weak reflections (vide infra). Sharp reflections were recorded at 1500 °C. Their patterns are attributable to a composite compound of the crystalline phases including $\beta\text{-Si}_3\text{N}_4$, SiC, and AlN. $\beta\text{-Si}_3\text{N}_4$ exists as an intermediate phase as no corresponding reflections were recorded at 1700 °C. The XRD patterns of the source powder pyrolyzed at 1700 °C are characteristic of the wurtzite structure. The measured d data give intermediate values between those of 2H–SiC and AlN, suggesting formation of a 2H–SiC/AlN solid solution.¹²

NMR. ^{29}Si and ^{27}Al MAS NMR spectra provide further information to elucidate the above crystallization sequence. ^{29}Si SP/MAS NMR analysis at 1100 °C (Figure 4) recorded the same spectral shape as the source powder (Figure 1b), which gives a broad strong resonance at -102.0 ppm (Q type). New spectral features

(25) van Wüllen, L.; Kalwei, M. *J. Magn. Reson.* **1999**, *139*, 250.

(26) Engelhardt, G.; Michel, D. *High-Resolution Solid-State NMR of Silicates and Zeolites*; John Wiley and Sons: Chichester, New York, 1987.

(27) Acosta, S.; Corriu, R. J. P.; Leclercq, D.; Mutin, P. H.; Vioux, A. *Mater. Res. Soc. Symp. Proc.* **1994**, *346*, 345.

(28) Fitzgerald, J. J.; Hamza, A. I.; Dec, S. F.; Bronnimann, C. E. *J. Phys. Chem.* **1996**, *100*, 17351.

(29) Kim, J. Y.; Kumta, P. N.; Phillips, B. L.; Risbud, S. H. *J. Phys. Chem. B* **2000**, *104*, 7895.

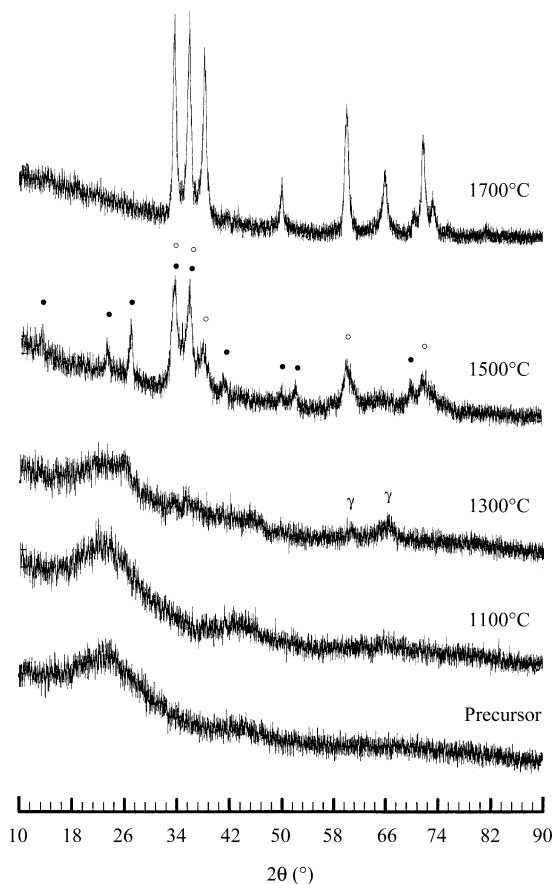


Figure 3. XRD patterns of the *source powder* and samples pyrolyzed at 1100, 1300, 1500, and 1700 °C: ● represents β - Si_3N_4 and/or β' -sialon with low z value; ○ represents AlN and SiC; and γ represents γ - Al_2O_3 and/or γ -AlON.

appear at 1300 °C, indicative of the occurrence of the structural change. In addition to the downward broadening of the Q type resonance, a broad strong resonance at -48.1 ppm is observed, attributable to SiN_4 sites, indicating formation of amorphous or poorly crystallized β - Si_3N_4 and/or β' -sialon phases as both give a very similar chemical shift value.^{30–32} Meanwhile, a very small peak in its downfield shoulder at ~ -18.5 ppm also suggests formation of SiC_4 sites of a short range order, i.e., amorphous SiC. At 1500 °C, this weak peak evolves into a much stronger resonance at -17.4 ppm, indicating the ordering of SiC_4 sites. Simultaneously, a sharp peak at -48.5 ppm replaces the broad one at 1300 °C, confirming formation of SiN_4 units with a long range order. Further absence of SiN_4 species was recorded at 1700 °C. Instead, a single and broad peak centered at ca. -19.0 ppm is the only recorded resonance in the final product. In contrast, the 2H polytype of SiC gives a sharp peak at -20.0 ppm³³ (vide infra).

Corresponding to the above structural evolution revealed by ^{29}Si NMR spectra, ^{27}Al MAS NMR spectra (Figure 5) provide additional information on the change in the local Al coordination environments. Quite differ-

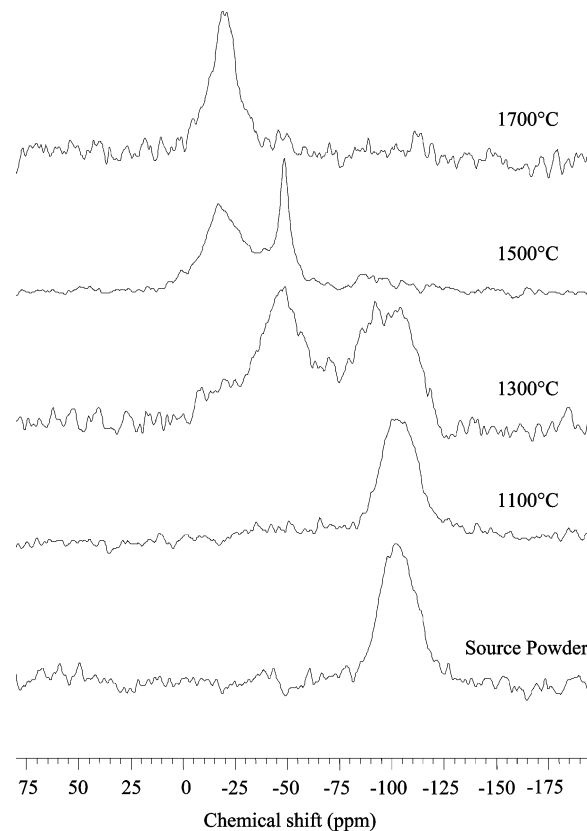


Figure 4. Solid-state ^{29}Si SP/MAS NMR spectra of the *source powder* and samples pyrolyzed at 1100, 1300, 1500, and 1700 °C.

ent from the evolutionary trend of AlAce/PS = 2.00 at temperatures ≤ 900 °C (Figure 2), the preferred development of pentahedral AlO_5 sites goes no further at 1100 °C. Instead, octahedral sites again become predominant in the pyrolyzed sample. At 1300 °C, complete disappearance of pentahedral AlO_5 sites was recorded. The ^{27}Al MAS NMR spectrum gives only two broad peaks at 52.1 ppm and -2.1 ppm, still assigned to AlO_4 and AlO_6 sites, respectively. This spectrum is similar with those of mullite and γ -phase (γ - Al_2O_3 and/or γ -AlON)^{27–29} (vide infra). At 1500 °C, a strong resonance centered at 111.6 ppm was recorded, attributable to AlN_4 sites of AlN.^{29,30} The formation of crystalline AlN is at the expense of AlO_6 and AlO_4 sites via carbothermal nitridation, as indicated by the simultaneous recording of a minor AlO_4 resonance and complete disappearance of AlO_6 sites which are the most intensive at 1300 °C. The upfield shoulder up to the AlN_4 resonance of the AlN₄ peak suggests the existence of mixed $\text{Al}(\text{O},\text{N})_4$ sites. At 1700 °C, only a single sharp resonance at 111.6 ppm was recorded, confirming progressive carbothermal nitridation of AlO_4 and mixed $\text{Al}(\text{O},\text{N})_4$ sites into AlN_4 .

Electron Microscopy. The microstructural evolution was further revealed by SEM and TEM observations. Typical morphological development is shown in Figure 6. The particles of the source powder (Figure 6a) are smooth and dense, but, in contrast, at 1500 °C, particles appear fragmented due to the occurrence of carbothermal reduction and nitridation (Figure 6b). The pyrolysis product at 1700 °C (Figure 6c) consists of aggregates of fine particles about $0.1 \mu\text{m}$ in size. TEM analysis confirms that the samples pyrolyzed up to

(30) Sjöberg, J.; Harris, R. K.; Apperley, D. C. *J. Mater. Chem.* **1992**, *2*, 433.

(31) Mackenzie, K. J. D.; Meinhold, R. H.; White, G. V.; Sheppard, C. M.; Sherriff, B. L. *J. Mater. Sci.* **1994**, *29*, 2611.

(32) MacKenzie, K. J. D.; Meinhold, R. H. *J. Mater. Chem.* **1994**, *4*, 1595.

(33) Apperley, D. C.; Harris, R. K.; Marshall, G. L.; Thompson, D. P. *J. Am. Ceram. Soc.* **1990**, *74*, 777.

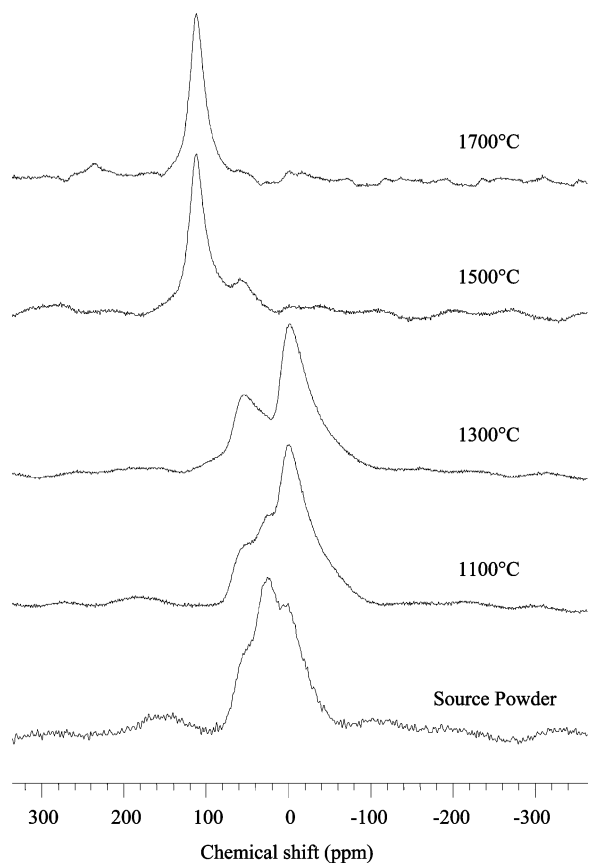


Figure 5. Solid-state ^{27}Al MAS NMR spectra of the *source powder* and samples pyrolyzed at 1100, 1300, 1500, and 1700 °C.

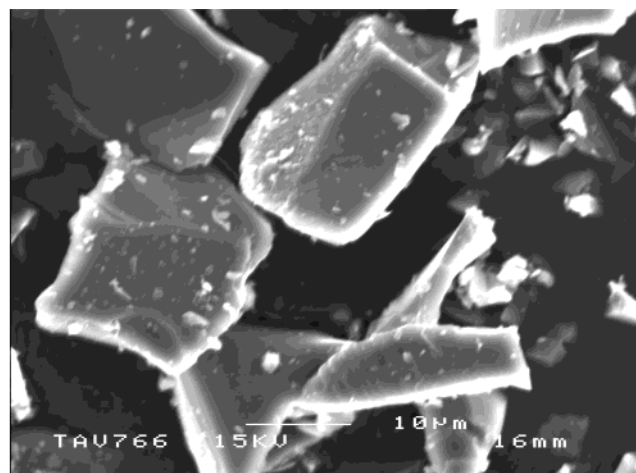
1100 °C remain amorphous. In addition to the presence of the main matrix consisting of fine particles, needlelike crystals were observed at 1300 °C (Figure 7) (*vide infra*). The bright and dark field images of the pyrolysis product at 1700 °C are shown in Figure 8. The grain size is ~ 50 nm. The corresponding selected area electron diffraction (SAED) is shown in Figure 8c. The rings consist of fine dark spots and correspond to the reflections of the wurtzite structure, confirming, on a nanometer scale, the formation of a solid solution of 2H–SiC and AlN.

Discussion

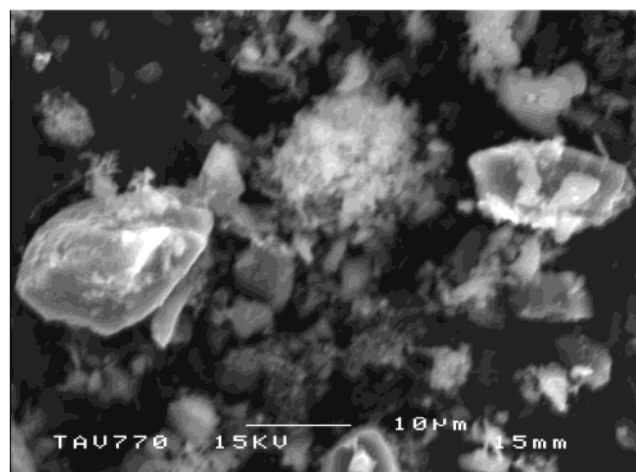
The polysilane used in this study is a terpolymer containing methyl, phenyl, and minor vinyl groups. Chemical reactions between PS and AlAce ($\text{Al}(\text{O}_2\text{C}_5\text{H}_7)_3$) change the Si moieties by introduction of Si–O bonds compared with only Si–Si and Si–C bonds of polysilane. Fourier transform infrared spectroscopy and NMR investigations of the precursors with varying AlAce/PS ratios confirm the scission of Si–Si bonds, cleavage of Si–phenyl bonds, and formation of Si–O, Al–O bonds and Si–O–Al linkages.^{12,34}

In this study, ^{29}Si NMR analysis of the precursor with AlAce/PS = 2.00 gives a spectrum featuring SiCO species, confirming the loss of the characteristic polysilane linkage which is indicated by an existence of ca. -39 ppm ^{29}Si peak.³⁴ In contrast to the unambiguous

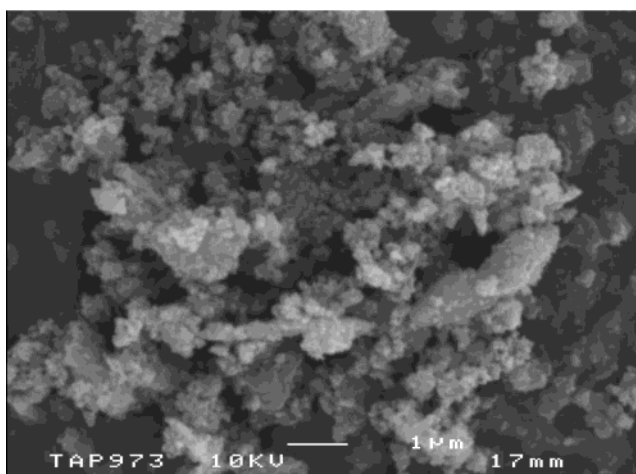
(34) Full NMR analysis of the precursors with varying AlAce/PS ratios will be described elsewhere.



(a)



(b)



(c)

Figure 6. Typical scanning electron micrographs of (a) source powder and samples pyrolyzed at (b) 1500 °C and (c) 1700 °C.

assignment of T and Q type units, the assignment and quantitative analysis of the overlapped signals to M and D type and SiC_4 sites are approximate due to the discrepancies in the assignment of these resonances in the literature.^{19,22–24} In fact, the existence of Si–Si bonds cannot be completely excluded as SiSiO_2Me units are located at -22 ppm and persist after heating at 500 °C, according to the chemical analysis by Belot et al.¹⁹

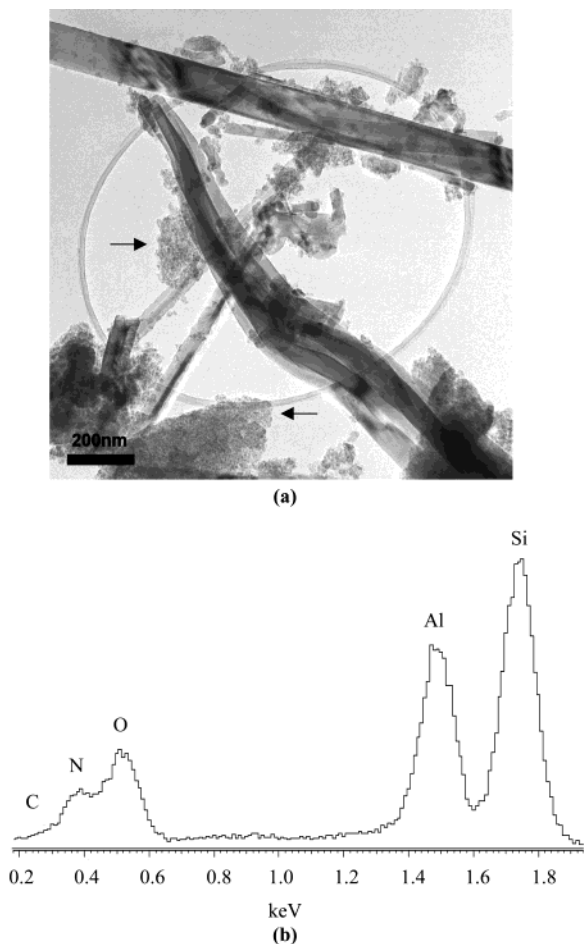


Figure 7. (a) Bright field image of the sample pyrolyzed at 1300 °C showing needlelike crystals and fine particles (see arrow) and (b) EDX spectrum of the needlelike crystals.

It is also noteworthy that the unit $\text{Si}(\text{C}_6\text{H}_5)_3\text{O}_3$ is positioned at -78 ppm.²² The absence of this signal in the T type units confirms the easy cleavage of Si–phenyl linkages during synthesis.¹² However, relevant deconvolution results provide useful information about the molecular structure of the precursor and its evolution during pyrolysis at temperatures ≤ 900 °C (Table 1).

The number of bridging oxygens surrounding the silicon atoms is denoted by using a superscript.²⁶ For example, Q^4 units represent a completely cross-linked silica, located at ca. -110 ppm.²⁹ Si chemical shifts are strongly influenced by next-nearest neighbors.^{19,22–24,26} Substitution of a Si–O–Si by Si–O–H or Si–OR linkage results in a downfield shift of ca. 10 ppm, while for each substitution of Si–O–Si by Si–O–Al bonds a downfield shift of ca. 5 ppm occurs.²⁶ Compared with the unresolved broad Q^n type units of the precursor at -104.0 ppm, the downfield shifting of Q type units at 500 °C is due to the formation of Si–O–Al bonds as the redistribution reactions usually lead to broadening and upfield shifting of the Si sites during the pyrolysis of SiCO species.^{19,24} The strong and broad Q type units centered at -93.1 ppm correspond to an average value of two to three Si–O–Al bonds.²⁷ Al NMR spectra recorded the proportional growth of AlO_4 and AlO_5 sites relative to AlO_6 sites in the pyrolyzed samples (Figure 2), supporting the incorporation of AlO_4 tetrahedral species into SiO_4 framework for Si–O–Al formation.

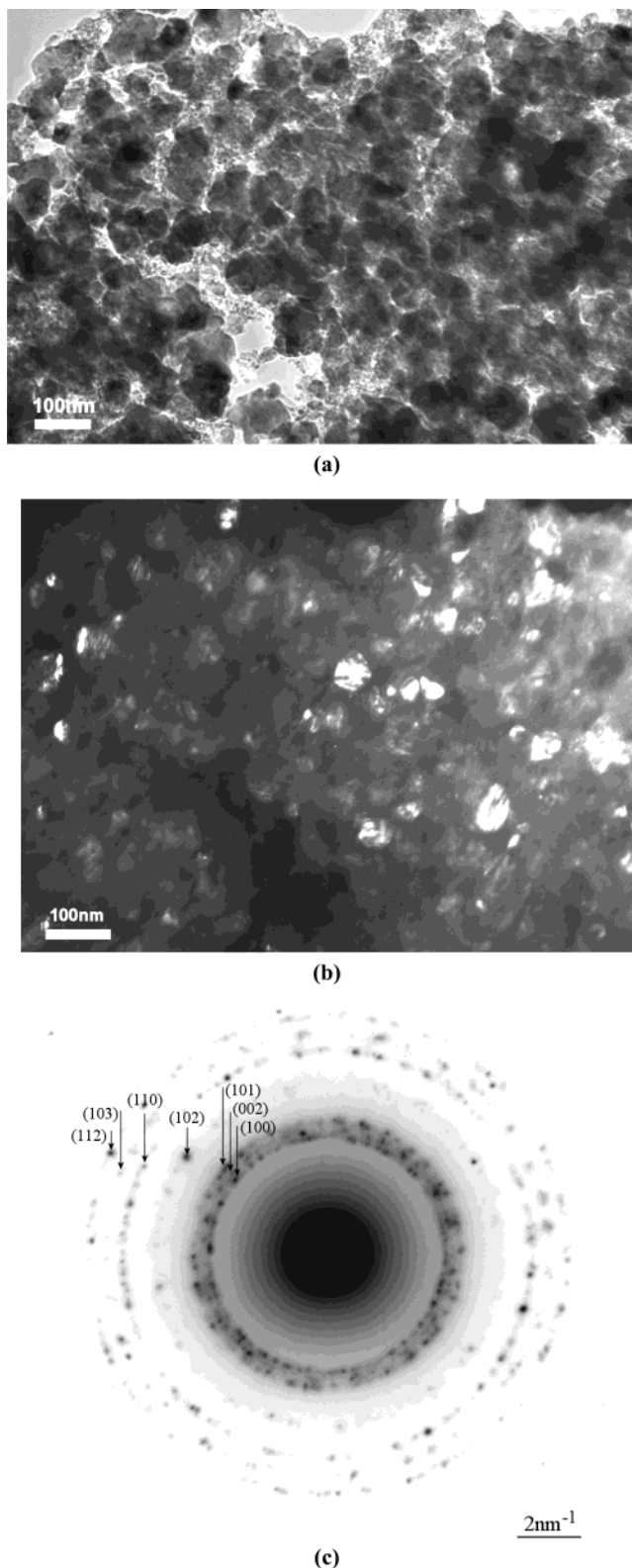


Figure 8. Transmission electron micrographs of the sample pyrolyzed at 1700 °C: (a) bright field image and (b) dark field image; and (c) corresponding selected area electron diffractions.

In contrast to the resolved Q^n peaks observed for amorphous silica,³⁵ the existence of Si–O–Al bonds in the precursor is also plausible, judged by the unresolved broad Q^n sites. In fact, the presence of Si–O–Al bonds in the precursor and the pyrolyzed samples is further

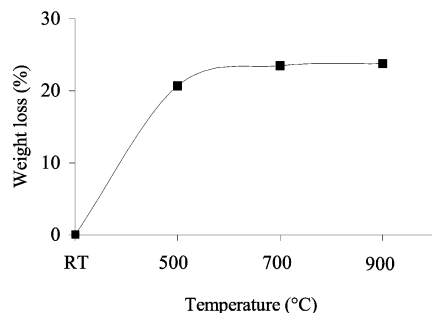
(35) Sindorf, D. W.; Maciel, G. E. *J. Am. Chem. Soc.* **1983**, *105*, 1487.

Table 1. Deconvoluted Results of ^{29}Si NMR Spectra of the Precursor on Pyrolysis to $\leq 900\text{ }^\circ\text{C}$

temperature	chemical shift (ppm) and the relative intensity (%) of different units									
	SiC_4		M type		D type		T type		Q type	
RT (precursor)	-2.9	14.2%	10.3	13.0%	-20.0	22.0%	-65.6	40.2%	-104.0	10.6%
500 $^\circ\text{C}$	-3.0	3.4%	8.5	5.6%	-18.4	7.6%	-61.5	31.0%	-93.2	52.4%
700 $^\circ\text{C}$							-67.8	10.9%	-93.9	89.1%
900 $^\circ\text{C}$									-101.0	100%

Table 2. Deconvolution of ^{29}Si NMR Spectrum of the Source Powder Pyrolyzed at 1300 $^\circ\text{C}$

component no.	1	2	3	4	5	6	7
chemical shift (ppm)	-111.1	-101.3	-87.7	-70.0	-55.9	-46.1	-18.5
relative intensity (%)	5.4	29.5	11.7	6.5	6.4	34.6	5.9
assignment ³⁷	SiO_4	Si–O–Al network	SiN_3O	SiN_2O_2	SiNO_3	SiN_4	SiC_4

**Figure 9.** Weight loss of the samples pyrolyzed at temperatures $\leq 900\text{ }^\circ\text{C}$.

consolidated by the upfield shift of AlO_4 sites detected in this study (51.3–55.4 ppm) relative to the reported values (65–70 ppm).⁵

Weight loss recorded during pyrolysis $\leq 900\text{ }^\circ\text{C}$ is given in Figure 9. The total loss at 900 $^\circ\text{C}$ is 25.2%. This value is quite low compared with 53.8% for the pyrolysis of pure polysilane. This is believed to arise from the incorporation of Si–O and Al–O bonds into the structure of polysilane and formation of Si–O–Al bonds during synthesis. In addition, it is evident that the heat treatment at temperatures $\leq 900\text{ }^\circ\text{C}$ leads to progressive development of a three-dimensional Si–O–Al network and the removal of organic ligands (see Table 1). Most of the weight loss was recorded at 500 $^\circ\text{C}$. This result corresponds to the significant change in the Si moieties, i.e., the downfield shifting and growth of Q type units at the expense of M and D type units and SiC_4 units, indicative of abrupt formation of Si–O–Al bonds. In fact, with increasing temperature oxygen continuously competes with carbon to bond to Si atoms. At 900 $^\circ\text{C}$, complete segregation of carbon from the network was evident (Table 1).

The XRD results^{12,36} revealed that the pyrolysis products of the precursors with low AlAce/PS ratio, such as 0.25, 0.50, are composites of AlN and SiC including the 2H and 3C polytypes and that the products of the precursors with higher AlAce/PS ratio such as 2.00 are presumably a solid solution of 2H–SiC and AlN as XRD data give intermediate *d* values. TEM analytical result (Figure 8c) verifies the formation of a solid solution in this study. Formation of AlN is further confirmed by the recording of a ^{27}Al peak at 111.6 ppm attributable to AlN_4 sites.^{29,30} However, ^{29}Si spectrum of the product at 1700 $^\circ\text{C}$ gives a broad peak including a component with the chemical shift value for pure 2H–SiC.³³ As is

known, ^{29}Si NMR chemical shifts of SiC are sensitive to the next-nearest neighbors. A broad ^{29}Si spectrum seems indicative of the existence of different SiC polytypes.

In fact, variant ^{29}Si chemical shift values for SiC–AlN ceramics were reported. For example, Interrante et al.⁴ reported that the gradually pyrolyzed precursor mixture of hydridopolycarbosilane and $[\text{Et}_2\text{AlNH}_2]_3$ gave a ^{29}Si peak at -17.2, whereas the corresponding rapidly pyrolyzed sample recorded a relatively broad peak centered at -24.5 ppm. They assumed that, on an atomic level, the achieved solid solution phases are slightly different. It seems, relative to the ^{27}Al NMR spectrum, that ^{29}Si NMR analysis provides extra information about the exact structure of the final SiC–AlN ceramics. The ^{29}Si NMR analysis of the pyrolysis products at 1700 $^\circ\text{C}$ of the precursors with varying AlAce/PS ratio by the present authors found downfield broadening of the ^{29}Si resonances of the products with the higher AlAce/PS ratio. Therefore, the broad ^{29}Si spectrum of the product at 1700 $^\circ\text{C}$ recorded in this study (Figure 4) is presumably related to a more solid-solution-like phase according to the corresponding XRD results.

As indicated above, the source powder is a three-dimensional Si–O–Al network with complete segregation of carbon. Accordingly, carbothermal reduction and simultaneous nitridation are expected to occur for crystalline phase formation with increasing temperature. Table 2 is the deconvoluted results of the ^{29}Si spectrum of the source powder pyrolyzed at 1300 $^\circ\text{C}$, confirming the formation of $\text{Si}(\text{N},\text{O})_4$ units³⁷ via bond redistribution and nitridation. The component at -101.3 ppm corresponds to the resonance attributable to the three-dimensional aluminosilicate network which was observed at 900 and 1100 $^\circ\text{C}$ (Figure 4). It accounts for 29.5%, indicating that about 70% of the Si–O–Al network has decomposed by 1300 $^\circ\text{C}$. The main decomposed component (49.1%) is located at -46.1 ppm, attributable to SiN_4 units. In fact, the initial information about carbothermal nitridation of the Si–O–Al network was detected by ^{29}Si NMR experiments at 1100 $^\circ\text{C}$, as indicated by the presence of an elevated background level upward from ca. -25 ppm (Figure 4). The existence of the SiC_4 component at -18.5 ppm indicates carbothermal reduction of silica at -111.1 ppm at this temperature.

(36) Li, X. D.; Edirisinghe, M. J. *J. Am. Ceram. Soc.* **2003**, *86*, 2212.(37) Gerardin, C.; Henry, M.; Taulelle, F. *Mater. Res. Soc. Symp. Proc.* **1992**, *271*, 777.

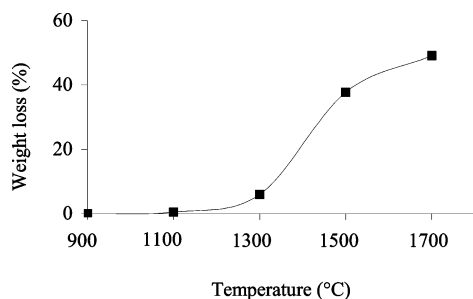


Figure 10. Weight loss of the source powder as a function of temperature.

In response to the decomposition of the -102.0 ppm ^{29}Si resonance, ^{27}Al NMR at 1300 °C recorded two peaks at 52.1 ppm and -2.1 ppm, associated with the AlO_4 and AlO_6 species. This spectrum is mainly ascribed to $\gamma\text{-Al}_2\text{O}_3$.²⁸ Formation of poorly crystallized γ -phase can be identified in the XRD patterns of the *source powder* pyrolyzed at 1300 °C (Figure 3). The weak and broad peaks at 66.3° and 60.7° are assigned to planes (440) and (333) of γ -phase.²⁹ In contrast to Si_3N_4 and SiC phases revealed by ^{29}Si NMR analysis, XRD results confirm the formation of $\gamma\text{-Al}_2\text{O}_3$ with a longer range order. Compared with the relatively stable Si–O–Al network up to 1300 °C (Figure 4), continual evolution of the local coordinations of Al atoms was actually recorded by ^{27}Al NMR analysis (Figure 5).

The reversed growth of AlO_6 sites relative to AlO_4 and AlO_5 sites at 1100 °C confirms the separation of the alumina phase from the Si–O–Al framework before final formation of $\gamma\text{-Al}_2\text{O}_3$ at 1300 °C. In fact, ^{27}Al NMR detected initial preferred growth of AlO_5 sites at 700 °C in contrast to the proportional growth of AlO_4 and AlO_5 sites relative to AlO_6 sites for formation of a three-dimensional Si–O–Al framework (Figure 2). This result suggests the occurrence of some structural changes in the system which need the AlO_5 sites as an intermediate environment to accommodate such alterations. This presumption is verified at 900 °C by both ^{29}Si and ^{27}Al NMR analyses. The most intensive AlO_5 sites correspond to the upfield shifting of Q type units to -101.0 ppm, indicating the partial disruption of Si–O–Al linkages. This evolutionary process of the Al local coordinations finally leads to the detection of the alumina phase separation at 1300 °C (Figures 3 and 5) when further heat treatment of the source powder is applied.

No XRD patterns are assigned to $\gamma\text{-Al}_2\text{O}_3$ phase at 1500 °C. Instead, strong reflections indicate the formation of a composite compound including $\beta\text{-Si}_3\text{N}_4$, SiC, and AlN. ^{29}Si NMR analysis confirms the complete decomposition of the Si–O–Al framework, ordering of SiN_4 sites, and formation and further ordering of SiC_4 sites. Carbothermal reduction and simultaneous nitridation of $\gamma\text{-Al}_2\text{O}_3$ was also detected by ^{27}Al NMR analysis, which leads to the formation of crystalline AlN. The occurrence of these significant structural changes is further revealed by SEM observation of the appearance of fragmented particles (Figure 6b).

The progression of carbothermal reduction and nitridation discussed above is verified by the recorded weight loss during pyrolysis as shown in Figure 10. Indication of weight loss at 1700 °C corresponds mainly to the decomposition of unstable Si_3N_4 phase under the presence of excess carbon together with continuous carbo-

thermal reduction and nitridation of AlO_4 and $\text{Al}(\text{O},\text{N})_4$ units into AlN_4 units with a long range order.³⁶ This final process leads to the formation of 2H-SiC-AlN solid solutions, as confirmed by ^{29}Si and ^{27}Al NMR, XRD, and electron microscopy.

In addition to the main reaction sequences revealed above, the existence of mullite and β' -sialon is also discussed. Mullite phase was reported as the main intermediate phase in the carbothermal conversion of an alumina, silica, and carbon mixture³⁸ and aluminosilicate minerals.³¹ The lack of this phase is assumed to be due to the existence of ample segregated carbon which forms an intimate contact with the Si–O–Al network.

β' -sialon ($\text{Si}_{6-z}\text{Al}_z\text{O}_z\text{N}_{8-z}$) is achieved in carbothermal nitridation of alumina, silica, and carbon mixtures, clay minerals, and preceramic precursors.^{18,31,38} Nakashima et al.¹⁰ also even detected the formation of β' -sialon during pyrolysis of cage-type and cyclic molecular building blocks into Al–Si–N–C ceramics under $\text{NH}_3\text{-N}_2$. In this study, compared with well-developed SiN_4 units at 1300 °C (Figure 4), it seems feasible that carbothermal reduction and nitridation of Al–O bonds into $\text{AlO}_x\text{N}_{4-x}$ tetrahedral sites would subsequently progress, followed by diffusion into SiN_4 for the β' -sialon phase. This inference was verified by TEM observation of needlelike crystals as shown in Figure 7. The corresponding EDX data (Figure 7b) suggest formation of β' -sialon with a substitution degree with $z \approx 1.0$. However, by studying the shifting of diffraction peaks recorded at 1500 °C using a long scan (0.02° step width, 10-s scan time per step, and 4-s delay time) with Si as an internal standard, a substitution of Si–N bonds by Al–O bonds was estimated from the measured unit cell parameters ($a = 0.76224$ nm, $c = 0.29238$ nm) according to the literature³⁹ and the substitution degree is very low at $z = 0.6$. The low substitution value recorded by XRD in samples heated to 1500 °C indicates the further occurrence of carbothermal reduction and nitridation of the β' -sialon formed. This process is supported by the reported NMR and XRD studies of sintering of Si_3N_4 using alumina as an additive.³² Therefore, it can be inferred in this study that gradual carbothermal nitridation of alumina, and subsequently diffusion into SiN_4 , generate β' -sialon and that, finally, formation of SiN_4 and AlN_4 by further nitridation happens with increasing temperature.

Conclusions

It was possible to study the structural evolution during thermal degradation of a Si–Al–C–O precursor with $\text{AlAce/PS} = 2.00$ as a function of temperature using solid state ^{29}Si and ^{27}Al NMR, XRD, and electron microscopy. The Si–Al–C–O precursor contained all the SiCO species (SiC₄, M, D, T, and Q units) and Si–O–Al linkages, resulting from chemical reactions between PS and AlAce, as revealed by NMR analysis. Pyrolysis at temperatures ≤ 900 °C leads to a three-dimensional Si–O–Al framework with the segregated carbon intimately dispersed in it. This evolution

(38) Sopicka-lizer, M.; Terpstra, R. A.; Metselaer, R. *J. Mater. Sci.* **1995**, *30*, 6363.

(39) Ekström, T.; Käll, P. O.; Nygren, M.; Olsson, P. O. *J. Mater. Sci.* **1989**, *24*, 1853.

is accompanied with the loss of organic ligands, and the resulting structural framework is stable up to 1100 °C.

Obvious decomposition occurs at 1300 °C, as indicated by notable SiN_4 units in the ^{29}Si NMR spectrum. A slight SiC_4 resonance was also detected. In contrast, ^{27}Al NMR spectrum gives resonances for $\gamma\text{-Al}_2\text{O}_3$. Strong reflections were observed at 1500 °C and the crystalline phases include $\beta\text{-Si}_3\text{N}_4$ and SiC and AlN. Compared with formation SiN_4 at 1300 °C, obvious carbothermal reduction and nitridation of Al–O bonds, mainly AlO_6 sites, occur at this temperature, as evidenced by a strong AlN_4 resonance and a weak AlO_4 resonance. The formation of some β' -sialon is expected by transformation of AlO_6 and AlO_4 sites into the Al(O,N)_4 sites during this process, but decomposition by further carbothermal

nitridation follows as a low substitution degree is recorded at 1500 °C by XRD analysis. The reaction of Si_3N_4 with the segregated carbon takes place at >1500 °C. This reaction, together with the conversion of small AlO_4 and Al(O,N)_4 sites to AlN_4 sites by continuous carbothermal reduction and nitridation, gives rise to the formation of SiC–AlN solid solutions at 1700 °C.

Acknowledgment. X.D.L. is sponsored by the Andrew Carnegie Research Fund of the Institute of Materials, Minerals and Mining, UK. Dr. A. E. Aliev and Mr. D. A. Butler of the Department of Chemistry of University College London are thanked deeply for their help with NMR work.

CM030584E